

## Hematotoxicity of magnetite nanoparticles coated with polyethylene glycol: *In vitro* and *in vivo* study

A. Ruiz<sup>a,b§</sup>, L. M. A. Ali<sup>c§</sup>, P. R. Cáceres-Vélez<sup>d</sup>, R. Cornudella<sup>e</sup>, M. Gutiérrez<sup>e</sup>, J. A. Moreno<sup>e</sup>, R. Piñol<sup>c</sup>, F. Palacio<sup>c</sup>, M. L. Fascineli<sup>d</sup>, R. B. de Azevedo<sup>d</sup>, M. P. Morales<sup>a\*</sup> and A. Millán<sup>c\*</sup>

Received  
Accepted

DOI: 10.1039/x0xx000000x

[www.rsc.org/](http://www.rsc.org/)

Hematotoxicity of magnetite nanoparticles coated with dimercaptosuccinic acid (DMSA) and polyethylene glycol (PEG) has been evaluated by determining their safety *in vitro* and *in vivo* in a rat model up to 30 days after administration of a single dose. The *in vitro* analysis consists on global plasma coagulation (PT, aPTT, Fibrinogen) and platelet aggregation tests while the hematotoxicity studies *in vivo* include a complete blood count and the possible genotoxic effects analysis in the bone marrow hematopoietic function. Prolonged aPTT values indicate higher anticoagulant effect for NP-DMSA compared with PEG-coated nanoparticles as a consequence of the higher surface charge of the former. The *in vivo* tests showed that these bioferrofluids do not cause genotoxic effects, affect erythropoiesis or increase the number of immature erythrocytes in the bone marrow at the analyzed dose. However, nanoparticles administration showed a significant effect on the leukocytes counts in animals treated with DMSA coated nanoparticles 24 h after injection. This response is not observed in animals treated with PEG modified nanoparticles which justifies the use of this polymer in biomasking strategies.

Keywords: magnetic nanoparticles, toxicity, PEG coated nanoparticles, blood, hematological parameters

### Introduction

Magnetic nanoparticles based on iron oxides are being used as contrast agents in magnetic resonance imaging (MRI). Clinical applications of these materials in drug delivery, hyperthermia and diagnosis are also being considered seriously<sup>1</sup>. However, a first requisite for *in vivo* applications is blood compatibility<sup>2</sup>, otherwise these materials would be immediately discarded for intravenous administration.

Interactions of nanoparticles with blood usually start with protein adsorption<sup>3</sup>, and subsequently derive in coagulation problems and other disturbances. Several studies have reported that environmental nanoparticles significantly increase the risk and worsen the prognosis of cardiovascular diseases due to the induction of thrombotic complications<sup>4</sup>. Protein adsorption is favored by surface charges, especially positive charges, and can be minimized with an appropriate coating. Carbohydrates and other biological polymers have been considered to be effective against protein adsorption, although polyethylene glycol is the preferred coating for these

## ARTICLE

purposes<sup>5, 6</sup>. However there are only few studies investigating the hematological effects of nanoparticles *in vivo* in spite of the fact that the majority of nanoparticle formulations are intended for systemic administration in clinical applications. In addition, there are no standard methodologies for the *in vitro* assessment of the blood compatibility of these nanoproducts.

The *in vitro* biocompatibility studies should also include evidence of hemolysis. The unique physicochemical properties of the nanoparticles could cause hemolysis by acting on the membrane of red blood cells. Several studies have revealed the effect of the nanoparticles on the blood by measuring their hemolytic action *in vitro*<sup>7</sup>. However, direct results interpretation of these studies is complicated due to variability of the experimental conditions such as incubation time of blood with the nanoparticles, the wavelength at which the hemoglobin is quantified, the centrifugation forces, blood storage time and conditions and blood source (human or rabbit)<sup>8</sup>.

Platelets are very sensitive to contact with biological substances, such as collagen, ADP and epinephrine, and non-biological ones, including ristocetin, that are commonly used in the hematology laboratory to detect functional defects of platelets. Foreign materials and high shear stress can also induce platelet aggregation. When this occurs they tend to produce micro aggregates that are easily detected by modern blood cell counters because they decrease the number of platelets and alter the size distribution curve. Nanoparticles can potentially damage the cell membrane and even the cytoplasm since they can penetrate inside cells. Blood cell counters not only quantify blood cells but also can detect abnormalities in shape, size and homogeneity.

This study was designed specifically to investigate whether iron oxide magnetite nanoparticles with a narrow size distribution (Mean size=7 nm; SD < 0.15) coated with different polymers

(Dimercaptosuccinic acid (DMSA) and Polyethylene glycol (PEG)) could lead to blood coagulation disorders and affect hematological parameters *in vitro* and *in vivo*. These bioferrofluids have previously been used in biodistribution and pharmacokinetics studies in different animal models. PEG coated nanoparticles have shown a good performance as MRI long circulating agents due to the effect of incorporation of PEG into the nanoparticle surface which is known to provide stealth coating to camouflage them, and thus, temporarily bypass recognition by macrophages<sup>9</sup>. As with any device or pharmaceutical product, DMSA or PEG coated nanoparticles intended for biomedical application must also be subjected to extensive blood biocompatibility testing before regulatory approval for administration to patients. To our knowledge, the blood biocompatibility of these products has not been established till date. Previous hematological studies on iron oxide nanoparticles coated with poly(4-vinyl pyridine)-polyethylene glycol (PVP-PEG) brush copolymers indicated a non-specific anticoagulant effect of the bioferrofluid<sup>10</sup>.

We have carried out an extensive *in vitro* biocompatibility study of our bioferrofluids with blood including coagulation studies, hemolysis and quantification of leukocytes, erythrocytes and platelets, to rule out immediate cytotoxicity of nanoparticles or contact spontaneous platelet aggregation<sup>11-13</sup>. Moreover, blood toxicity of these nanomaterials has been studied in terms of global tests (Prothrombin time (PT), activated partial thromboplastin time (aPTT), Fibrinogen), thrombus-elastography, platelet aggregation and degradation products of fibrinogen and fibrin. Recently, a detailed description of methods has been published, which focuses on the global plasma coagulation tests (PT, aPTT, Fibrinogen) and platelet aggregation<sup>14</sup>. The doses used in this study are higher than the therapeutically relevant concentration but describe the range where we observed an effect on hematological parameters. The

## Journal Name

recommended dosage for products like Feridex IV, Berlex Laboratories; and Endorem, Guerbet is 0.56 mg of iron per kg of body weight<sup>15</sup>. It is also in the same range as those used in other cytotoxicity assays published previously<sup>16</sup>.

Some studies have evaluated the compatibility of nanoparticles with the blood coagulation system<sup>17</sup> *in vivo* in rats<sup>18</sup> and rabbits<sup>19</sup>, while most of the authors have carried out only *in vitro* tests<sup>10-12, 20</sup>. Finally, we have carried out hematotoxicity studies *in vivo* including a complete blood count analysis and also possible genotoxic effects in the hematopoietic function of the bone marrow.

### Materials and methods

**Materials:** Iron (III) acetylacetonate, 1,2-dodecanediol, oleic acid, oleylamine, 1-octadecene, hexane, dimercaptosuccinic acid, ethanol, toluene, 1-ethyl-3-(3-dimethylaminopropyl) carbodiimide hydrochloride and O,O-bis(2-aminoethyl)-polyethylene glycol 2000 Da were commercial products purchased from Sigma-Aldrich. Female Wistar rats (from 10-13 weeks old) weighing 300 g  $\pm$  20 g were purchased from CEMIB (Campinas), and were maintained under controlled conditions before and during the experiments (*i.e.*, room temperature at 25 °C; relative humidity of 65 %; 12 h light/dark cycle) in the Institute of Biological Science (University of Brasília) animals' facility. Access to food and water was provided *ad libitum*. The present animal research was approved by the Animal Ethics Committee of the University of Brasília, Brazil. For *in vitro* studies blood samples were obtained from healthy human volunteers.

### Magnetic nanoparticles preparation

Magnetite nanoparticles were obtained *via* thermal decomposition of an iron coordination complex as a precursor to ensure nanoparticle

homogeneity in size and shape following the method reported by Sun and co-workers<sup>21, 22</sup>. Particle size and shape were studied using a 200 keV JEOL-2000 FXII microscope. A drop of a dilute magnetic nanoparticle suspension in hexane was placed on a carbon coated copper grid and dried at 50°C. Size distribution was determined through manual measurement of more than 200 particles and data were analyzed with Gwyddion 3.25 software to obtain the mean size and standard deviation by gaussian fitting. The superparamagnetic behavior of the nanoparticles was verified using a vibrating sample magnetometer (MLVSM9 MagLab 9T, Oxford Instruments). Magnetization curves were recorded by saturating the sample in a 5 T field at room temperature and sweeping the field range between 5 and -5 T at 0.3 T/min.

Particles were coated with meso-2,3-dimercaptosuccinic acid (NP-DMSA) by a ligand exchange reaction to remove oleic acid, after which a short-chain diamine PEG was covalently bound to the nanoparticle surface *via* 1-ethyl-3-(3-dimethylaminopropyl)-carbodiimide hydrochloride (EDC) activation of the carboxylic acids (NP-PEG-(NH<sub>2</sub>)<sub>2</sub>). Colloidal properties of 0.5 mM Fe nanoparticle suspensions in water were characterized by dynamic light scattering (DLS) using a Nanosizer ZS (Malvern). Z-Average values in intensity at pH 7 were used as the mean hydrodynamic size. The polydispersity degree index (PDI) was calculated by dividing the standard deviation by the mean size. The Z potential was measured in a 0.01 M KNO<sub>3</sub> solution. Other properties of NP-DMSA and NP-PEG-(NH<sub>2</sub>)<sub>2</sub> have been described in detail in previous publications<sup>16</sup>.

### Coagulation Studies

**Control plasma:** Blood samples were obtained from healthy human volunteers. Samples were collected in citrate (0.129 M) vacutainer tubes. The samples were centrifuged at 3500 rpm to obtain platelets-poor plasma (PPP). The plasma was processed for the coagulation

## ARTICLE

studies of aPTT and PT using the coagulometer TOP-ACL-TOP 700 from IL-Instrumentation. The results were within the reference limits (23-37 s. and 9-14 s. respectively).

**PPP treated with bioferrofluids:** NP-DMSA and NP-PEG-(NH<sub>2</sub>)<sub>2</sub> were mixed with PPP making serial dilutions for final particle concentrations ranging from 0.3 to 0.05 g/L of iron, and processed for the measurement of PT and aPTT. Blank samples of DMSA and DMSA-PEG-(NH<sub>2</sub>)<sub>2</sub> were prepared containing similar concentration of these reactants as those in bioferrofluid samples.

In order to find out the origin of the anticoagulant effect, samples that showed an increase of aPTT were tested by mixing them with normal plasma (mixing study), after that thrombin time and coagulation factors were measured. Fibrinogen was measured by von Clauss method in PPP treated with bioferrofluids at high concentration (0.3 g/L Fe) using reactants and the coagulometer TOP-ACL both from IL-Instrumentation Laboratory.

#### Complete blood counts (CBC) studies

**Control blood:** Blood samples were obtained from healthy human volunteers. Samples were collected in EDTA K3, 1.8 mg/mL vacutainer. The blood samples were processed for CBC studies using a Coulter LH 780 analyzer from Beckman Coulter.

**Blood treated with bioferrofluids:** the investigated materials were mixed with the blood samples at dilutions 1:10 and 1:100 and processed for blood cell counting.

#### Hemolysis studies

Blood samples were obtained from healthy human volunteers. Samples were collected in Lithium heparin 17 UI/mL vacutainer tubes. The samples were processed for the measurement of the free

hemoglobin using a double beam spectrophotometer Analytic Jena-Specord 205 with wavelength range between 500-630 nm.

#### Hematology analysis *in vivo*

Rats were randomly divided into three groups (n= 4/group), the control and the experimental groups: Animals treated with NP-DMSA and animals treated with NP-PEG-(NH<sub>2</sub>)<sub>2</sub>. The animals of the experimental groups received a single dose of magnetite nanoparticles (2.5 mg/kg B.W.) through the tail vein. This dose is five times larger than the recommended one for commercial products (~0.5 mg/kg B.W.)<sup>14</sup> but it is well below the doses used in many experimental works (10 mg/kg B.W.)<sup>23</sup>. Rats were anesthetized with a mixture of Ketamine/Xylazine and peripheral blood was collected at 24 hours, 7, 15 and 30 days after nanoparticles administration. Control animals were sacrificed progressively during the study. Blood collected in EDTA (10 %) was analyzed using a Sysmex pocH-100i™ Automated Hematology Analyzer.

#### Genotoxicity test

**Comet Assay:** The extent of DNA damage was determined *via* alkaline single cell gel electrophoresis according to N.P. Singh and cols.<sup>24</sup> with some modifications. Briefly, 60 μL of peripheral blood was mixed with 240 μL of 0.5% low melting point agarose. The mixture was pipetted into slides (2 slides/rat) precoated with 1.5% normal melting point agarose and covered with a coverglass. Then, the slides were incubated in freshly prepared lysis buffer (NaCl 2.5 M, EDTA 100 mM, Tris 10 mM, 1% Triton x-100, 10% DMSO) in the dark for 2 h at 4°C. The slides were then placed in a horizontal electrophoresis tank containing fresh electrophoresis buffer (300 mM NaOH, 1 mM EDTA, pH 13) and incubated for 30 min at 4°C. Electrophoresis was conducted for 30 min at 25 Volts and 300 mA. The slides were washed with neutralization solution (0.4 M Tris-HCl, pH 7.5) and stored at 4°C until analysis. Scoring was carried

## Journal Name

out under blinded conditions by an individual not connected with the study. The slides were stained with 60  $\mu\text{L}$  of ethidium bromide (20  $\mu\text{g}/\text{mL}$ ), coverslipped and cells were analyzed using a fluorescence microscope (ZEISS Axioskop 2-HAL 100) where 150 cells/rat were examined and classified. The cells were classified, according to the size and proportion nucleoid-tail<sup>25</sup>, in levels of damage observed (0, 1, 2, 3 and 4) to calculate the percentage of Total Damage (% TD) from Damage Index (DI) proposed by<sup>26</sup>.

**Cytotoxicity and Micronucleus test:** Bone marrow samples were suspended in fetal bovine serum (FBS). The suspension was homogenized and then centrifuged at 1000 rpm for 10 minutes. The supernatant was removed and the pellet was resuspended in 50  $\mu\text{L}$  of FBS. The smear was performed with 10  $\mu\text{L}$  of homogenate per slide (2 slides/rat). Slides were air-dried at room temperature, fixed with methanol (10 min) and stained with Giemsa at 20% (12 min). The stained slides were analyzed with a light microscope Olympus BH2. For each animal, 4000 cells were counted with a manual counter. The frequency of micronuclei was evaluated in 2000 polychromatic erythrocytes (PCE) and 2000 normochromatic (immature) erythrocytes (NCE), according to the OECD guideline 474 (1997). Cytotoxicity was assessed by the percentage of polychromatic erythrocytes PCE (% PCE); therefore, at the time of the populations of erythrocytes reached the mark of at 2000 cells during counting, the quantities of NCE and PCE were recorded and PCE% was calculated using the formula:

$$\%PCE = \frac{PCE}{PCE+NCE} \times 100$$

**Statistical analysis**

Data were analyzed by parametric or non-parametric statistics, according to the normal distribution using the Kolmogorov-Smirnov test. For parametric data was performed Analysis of Variance

(ANOVA) followed by Dunnett Multiple Comparisons test or t- test and nonparametric data were analyzed with the Mann-Whitney test. Statistical analysis data are summarized in Supplementary Material.

**Results and Discussion****Particle Characterization**

Iron oxide nanoparticles used in this work were obtained *via* thermal decomposition of iron (III) acetylacetonate in 1-octadecene in the presence of oleic acid. Particles were 7.5 nm in diameter, uniform in size (PDI = 0.16), relatively spherical and well dispersed due to the presence of oleic acid around the particles (Figure 1 A). To study the magnetic properties of the nanoparticles, magnetization curves were performed for the NP-oleic acid in hexane. The sample showed a superparamagnetic behavior with saturation magnetization values of 67 emu/ g Fe (Figure 1B). This is an important advantage that enables nanoparticle stability and dispersion upon removal of the magnetic field as no residual magnetic force exists between the particles. Several biomedical and bioengineering applications require that nanoparticles have high magnetization values and hydrodynamic size smaller than 100 nm with overall narrow particle size distribution, so that the particles have uniform physical and chemical properties.

Particles were coated with meso-2,3-dimercaptosuccinic acid (NP-DMSA) after a ligand exchange reaction. In order to increase the biocompatibility of the material NP-DMSA were chemically modified with PEG (NP-PEG-(NH<sub>2</sub>)<sub>2</sub>). Properties of NP-DMSA and NP-PEG-(NH<sub>2</sub>)<sub>2</sub> have been extensively described in previous publications<sup>9, 16</sup>. DLS observations showed a monomodal distribution of DMSA coated particles with an average hydrodynamic diameter of 22 nm and polydispersity degrees (PDI)

## ARTICLE

lower than 0.25. After PEG modification average hydrodynamic size at pH 7 is increased from 22 to 27 nm. Surface charge decreased from approximately -35 mV for NP-DMSA samples to values between -15 mV for PEG-modified nanoparticles (Figure 1 C, D). Nanoparticle size and surface chemistry and charge have a profound effect in the pharmacokinetic, biodistribution and toxicology of the product.

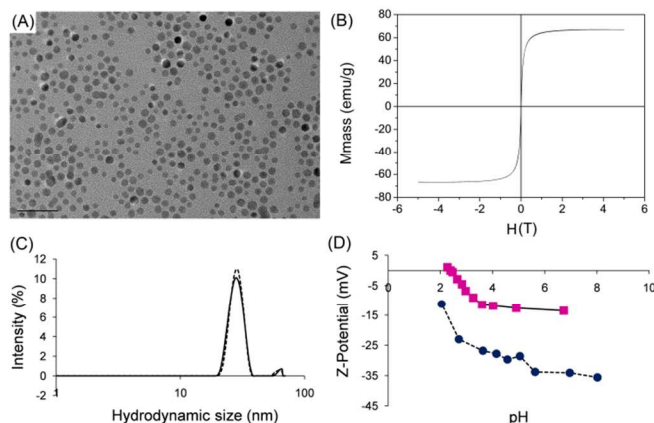


**Figure 1.** Nanoparticle Characterization. (A) Transmission electron microscopy images of  $\sim 7$  nm oleic acid coated nanoparticles. (B) Magnetization curve at 250 K for oleic acid coated nanoparticles. (C) Hydrodynamic sizes for NP-DMSA (solid line) and PEG coated nanoparticles (dotted line). (D) Evolution of Z-potential as a function of pH. NP-DMSA [●], NP-PEG-(NH<sub>2</sub>)<sub>2</sub> [■].

### Coagulation studies for DMSA and PEG coated bioferrofluids

The prothrombin time (PT) is a measurement of the extrinsic coagulation pathway, whereas the activated partial thromboplastin time (aPTT) is an indicator of the efficacy of both the intrinsic (now referred to as the contact activation pathway) and the common coagulation pathways. Both PT and aPTT were measured on PPP treated with different concentrations of NP-DMSA or NP-PEG-(NH<sub>2</sub>)<sub>2</sub> bioferrofluids ranging from 0.05 g/L Fe to 0.3 g/L Fe.

In the case of NP-DMSA treated plasma, the PT values are within our laboratory normal reference range (9-14 s). In general, they are slightly lower than control values. These results are plotted in Figure 2A. On the other hand, the aPTT shows a rapid increase as the NP-DMSA concentration increases. For instance, at the lowest concentration, 0.05 g/L Fe, aPTT value is already  $40.66 \pm 5.23$  s, significantly higher than the control one that is  $29.17 \pm 2.01$  s, and at the highest concentration, 0.3 g/L Fe, aPTT value is  $65.58 \pm 6.13$  s, more than double of the control value (Figure 2B).

In the case of NP-PEG-(NH<sub>2</sub>)<sub>2</sub> treated plasma, PT shows no significant difference for all concentrations tested (Figure 2A). Even at the highest concentration, 0.3 g/L Fe, the PT value is  $11.78 \pm 1.95$  s that compares well with its control value  $10.60 \pm 1.26$  s. In contrast, aPTT shows a significant concentration-dependent increase in the whole Fe concentration range (Figure 2B), although, at concentrations of 0.07 g/L Fe and below, the aPTT values are still within the laboratory normal reference range (29-37 s). At the highest concentration, 0.3 g/L Fe, aPTT value is already  $49.37 \pm 8.71$  s, well above the control value  $29.41 \pm 2.86$  s.

A prolonged aPTT suggests one of the following possibilities: a) deficiency of one or more coagulation factors; or b) presence of an inhibitor in plasma. The usual procedure to elucidate which of the two options is ruling consists on mixing the abnormal plasma (plasma treated with nanoparticles) with normal plasma and then measuring the aPTT again. If the prolongation of aPPT disappears, there is a deficiency of one or more coagulation factors. When the aPPT prolongation persists, it is indicative of the presence of an inhibitor. In the latest case, it is important to find out if the inhibition effect is specific or non-specific using new tests, including thrombin time (TT) and quantifying the activity of factors that may be affected by the inhibitor at various dilutions.

## Journal Name

In order to explore the cause of the aPTT prolongation, PPP treated with the highest concentration (0.3 g/L Fe) of NP-DMSA or NP-PEG-(NH<sub>2</sub>)<sub>2</sub> were used for the following studies: a) mixture tests, in which PPP treated with bioferrofluids were mixed with normal plasma (1:1), b) thrombin time (TT) measurements; and c) intrinsic coagulation factors (FVIII, FIX, FXI, and FXII) measurement.

In the case of NP-DMSA treated plasma, it was observed that: a) the aPTT measurements for bioferrofluids treated plasma, returned to

normal levels,  $30.83 \pm 0.74$  s after mixing with normal plasma (1:1); b) The TT values were also normal;  $27.83 \pm 2.57$  s compared to a control value of  $21.83 \pm 1.45$  s (TT reference limits is 15-28 s.); c) and intrinsic coagulation factors decreased, from  $126.70 \pm 4.10$  %,  $107.60 \pm 26.87$  %,  $79.00 \pm 11.46$  %,  $80.90 \pm 0.42$  % in the control to  $86.95 \pm 8.56$  %,  $63.05 \pm 15.20$  %,  $40.95 \pm 6.58$  % and  $37.55 \pm 4.45$  % in the treated one for FVIII, FIX, FXI, and FXII, respectively.

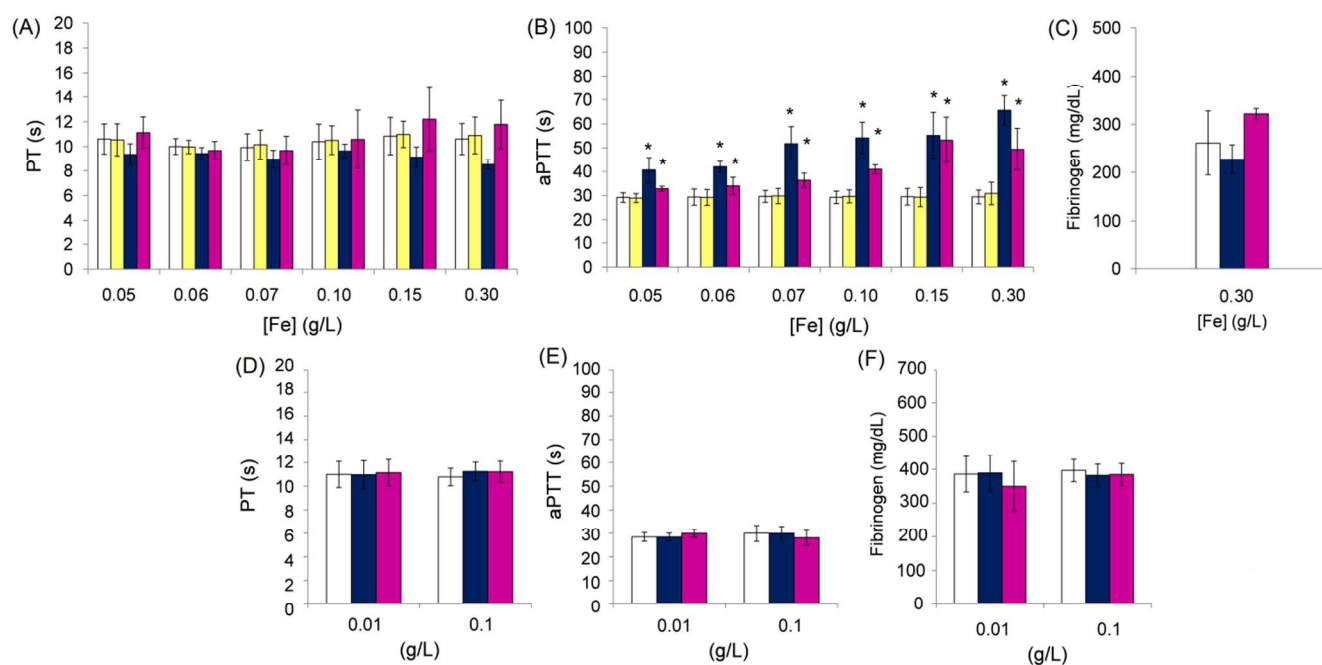


**Figure 2.** The effect of NP-DMSA and NP-PEG-(NH<sub>2</sub>)<sub>2</sub> on coagulation system: (A) Prothrombin time (B) Activated partial thromboplastin time, in seconds. Values represent mean  $\pm$  SD (n= 6 for bioferrofluids, 12 for PBS and 24 for control), (\*) marks significant differences between bioferrofluids and control. (C) The effect of NP-DMSA and NP-PEG-(NH<sub>2</sub>)<sub>2</sub> on the von Clauss determined Fibrinogen in mg/dL. Values represent mean  $\pm$  SD (n=3 for bioferrofluids, and 6 for control). The effect of DMSA and PEG-(NH<sub>2</sub>)<sub>2</sub> on coagulation system as free components: (D) Prothrombin time in seconds, (E) Activated partial thromboplastin time in seconds, and (F) Fibrinogen D in mg/dL. Values represent mean  $\pm$  SD (n=6 for DMSA and PEG-(NH<sub>2</sub>)<sub>2</sub>, and 12 for control). Control [□], PBS [■], NP-DMSA [■], NP-PEG-(NH<sub>2</sub>)<sub>2</sub> [■].

In the case of NP-PEG-(NH<sub>2</sub>)<sub>2</sub> treated plasma a similar trend was observed: a) the aPTT values returned to normal levels ( $33.40 \pm 1.73$  s (mean  $\pm$  SD) in the treated samples as compared to  $29.33 \pm 2.60$  s); b) TT measurements also showed normal values ( $28.37 \pm 1.59$  s in the PPP treated with NP-PEG-(NH<sub>2</sub>)<sub>2</sub>; as compared to  $24.03 \pm 0.50$  s in the control; and c) intrinsic coagulation factors decreased from  $99.50 \pm 31.54$  %,  $110.05 \pm 19.73$  %,  $90.75 \pm 2.90$  %,  $81.80 \pm 12.59$  % in control samples to  $54.00 \pm 16.55$ %,  $50.00 \pm 4.10$ %,  $50.25 \pm 3.18$  %,  $54.05 \pm 9.83$ % in treated samples, for FVIII, FIX, FXI, and FXII.

The prolonged aPTT values are probably due to an inhibition of intrinsic coagulation factors after nanoparticle addition<sup>27</sup>. When nanoparticles are in contact with a biological fluid their surface will be covered with a "corona" of biological macromolecules. Surface charge plays a fundamental role in this process, and this is evidenced by a higher inhibition effect of NP-DMSA compared with PEG-coated nanoparticles.

#### Fibrinogen measurements by von Clauss method

To avoid the possible interference of the suspended nanoparticles on the fibrinogen derived method, which is based on light dispersion, the von Clauss method was also used. The resulting measurements for PPP treated with NP-DMSA or NP-PEG-(NH<sub>2</sub>)<sub>2</sub> at the highest concentration (0.3 g/L Fe), showed no significant difference with respect to control (Figure 2C). Fibrinogen values were  $227.67 \pm 30.07$  mg/dL and  $321.67 \pm 10.97$  mg/dL for NP-DMSA and NP-PEG-(NH<sub>2</sub>)<sub>2</sub> treated plasma respectively, and  $261.33 \pm 66.48$  mg/dL for the control, which are not significantly different.

Taking together all these results (normal Fibrinogen values, normal values of intrinsic coagulation factors (FVIII, FIX, FXI, and FXII) and the factors in the common coagulation pathway), a possible case of Disseminated Intravascular Coagulation (DIC)-like toxicity *in vivo* can be discarded. It is also necessary to emphasize that the coagulation study was performed using a nanoparticles' amount much higher than those used in clinical applications.

#### Coagulation studies for separated components (DMSA and PEG-(NH<sub>2</sub>)<sub>2</sub>)

For this purpose, DMSA and PEG-(NH<sub>2</sub>)<sub>2</sub> blank samples were prepared. Thermogravimetric analysis previously reported<sup>16</sup> allows the preparation of different samples containing similar concentration of these compounds as those present in the nanoparticles. These solutions were mixed with PPP in different concentrations: 0.01 and 0.1 g/L (10 times higher than the amount present in the nanoparticles surface) of DMSA or PEG-(NH<sub>2</sub>)<sub>2</sub>, and none of them showed significant differences in terms of PT, aPTT and Fibrinogen by derived method with the control (Figure 2 D-F).

#### Complete blood counts (CBC) studies

Whole blood was treated with different concentrations (0.05 and 0.1 g/L Fe) of NP-DMSA and NP-PEG-(NH<sub>2</sub>)<sub>2</sub>, and processed for CBC measurements. The CBC (erythrocytes, leukocytes, platelets, hemoglobin and hematocrit) results did not show significant differences between control samples and blood treated with both bioferrofluids at both concentrations. Results are shown in Figure 3



(A-E). No significant differences in either hemoglobin or hematocrit were observed.

The spectrophotometric study of hemoglobin in plasma demonstrated the absence of hemolysis for both bioferrofluids at these concentrations (0.05 and 0.1 g/L Fe). Altogether these data show the nanoparticles safety related to erythrocytes. Similar results were found with respect to platelets and leukocytes as the instrument did not show any flags indicating morphologic alterations or aggregation in any of them, reinforcing the safety of nanoparticles.

The normal morphology of the cells was also confirmed by optical

microscope for stained blood films (Figure 4 A-F). Hemolysis could lead to the loss of the red blood cells characteristic biconcave shape and spherocytes formation. In our case, we did not observe smaller and denser cells than their normal counterparts in the samples treated with nanoparticles.

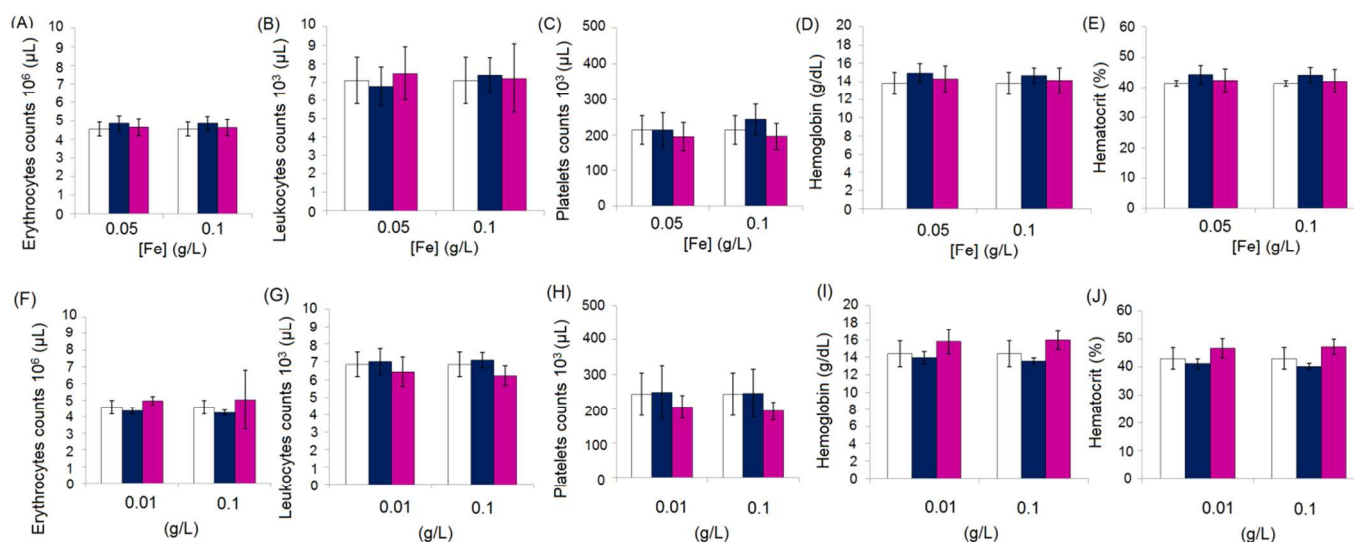


**Figure 3.** The effect of NP-DMSA and NP-PEG-(NH<sub>2</sub>)<sub>2</sub> on hematological parameters: (A) Erythrocytes, (B) Leukocytes, (C) Platelets, (D) Hemoglobin and (E) Hematocrit. Values represent mean ± SD (n=6 for bioferrofluids and 12 for control). Effect of DMSA and PEG-(NH<sub>2</sub>)<sub>2</sub> as free components in hematological parameters: (F) Erythrocytes, (G) Leukocytes, (H) Platelets, (I) Hemoglobin and (J) Hematocrit. Values represent mean ± SD (n=4 for DMSA and PEG-(NH<sub>2</sub>)<sub>2</sub> and 8 for control). Control [□], NP-DMSA [■], NP-PEG-(NH<sub>2</sub>)<sub>2</sub> [■].

### CBC studies for bioferrofluids separated components (DMSA and PEG-(NH<sub>2</sub>)<sub>2</sub>) **In vivo studies**

Whole blood was treated with different concentrations (0.01 and 0.1 g/L) of DMSA and PEG-(NH<sub>2</sub>)<sub>2</sub>, and processed for CBC measurements. The CBC (erythrocytes, leukocytes, platelets, hemoglobin and hematocrit) results did not show significant differences at both concentrations for blood treated with both materials and control. Results are shown in Figure 3 (F-J).

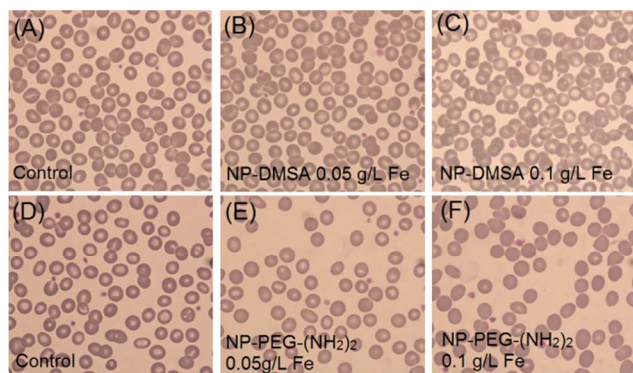


**Figure 4.** Cell morphology in presence of the nanoparticles: (A, D), Stained films of untreated blood and treated blood with NP-DMSA (upper panel) and NP-PEG-(NH<sub>2</sub>)<sub>2</sub> (lower panel) at concentrations 0.05 g/L Fe (B, E) and 0.1 g/L Fe (C, F).

### Hemolysis studies for blood treated with NP-DMSA and NP-PEG-(NH<sub>2</sub>)<sub>2</sub>

Whole blood was treated with different concentrations (0.05 and 0.1 g/L Fe) of NP-DMSA and NP-PEG-(NH<sub>2</sub>)<sub>2</sub>, hemolysis tests did not show any hemolytic effect observed with naked eyes. Spectrophotometric measurements did not show any peak referred to the free hemoglobin at wavelength 580 nm as shown in Figure 5. These curves were consistent with their control. These results are in agreement with CBC results presented above.

The influence of DMSA and PEG coated nanoparticles in hematological parameters was tested in a Wistar rat animal model up to 30 days after administration at a single dose of 2.5 mg/kg B.W. Complete blood counts are summarized in Figure 6. It was observed a slightly decrease in erythrocytes counts after 24 h. Nanoparticles administration also showed significant differences with the control in the leukocytes counts in animals treated with DMSA coated nanoparticles at 24 h after injection. This response is not observed in animals treated with PEG modified nanoparticles. Immobilization of PEG on surfaces is known to decrease protein adsorption and subsequent immune cells recruitment. Many models have been proposed to explain the mechanisms involved, but steric stabilization and charge shielding are the most commonly accepted. Thus, chemical groups on the surface of the nanoparticles such as those provided by the DMSA have shown protein adsorption and subsequent adhesion of monocytes/macrophages<sup>28</sup>. However, covalent conjugation of PEG to the free carboxyl group of DMSA masks surface charge (as indicated by a near neutral zeta potential) and creates a hydrophilic barrier that sterically prevents protein adsorption, reduces immunological recognition, and consequently the leukocyte count is not affected. This result justified the use of this polymer in biomasking strategies.

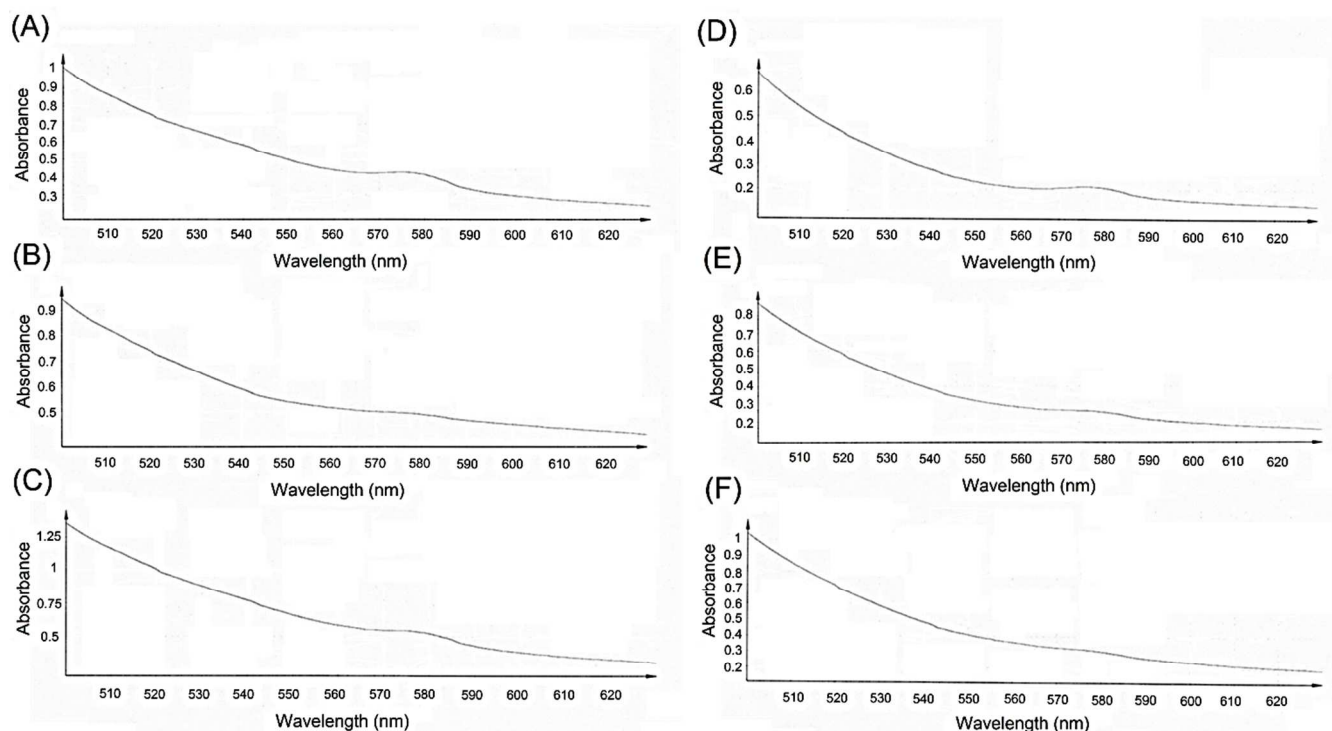


**Figure 5.** Hemolysis detection using spectrophotometer: (A,D) blood control, (B,C) blood treated with NP-DMSA at concentration 0.05 g/L and 0.1 g/L Fe respectively. (E) blood treated with NP-PEG-(NH<sub>2</sub>)<sub>2</sub> at concentration 0.05 g/L Fe and (F) blood treated with NP-PEG-(NH<sub>2</sub>)<sub>2</sub> at concentration 0.1 g/L Fe.

### Genotoxicity test

Many studies have shown that nanoparticles generate reactive oxygen species, deplete endogenous antioxidants, alter mitochondrial function and produce oxidative damage in DNA<sup>29</sup>. Single Cell Gel Electrophoresis assay (also known as Comet Assay) and Micronucleus test were performed in order to analyze possible hematotoxicity and genotoxicity associated to magnetite nanoparticles administration in a Wistar rat animal model<sup>30, 31</sup>. Electrophoresis at high pH allows detection of single and double strand DNA breaks, alkali-labile sites (expressed as single-strand breaks), single-strand breaks associated with incomplete repair, and DNA–DNA or DNA–protein cross-links<sup>24, 32</sup>. On the other hand Micronucleus test detects irreversible structural damages, for

example, chromosomal damages<sup>33</sup>. Total damage (TD %) and micronucleus frequencies showed no significant differences between the animals treated and control groups (Figure 7A) concluding that these bioferrofluids do not cause genotoxic effects at the analyzed dose.

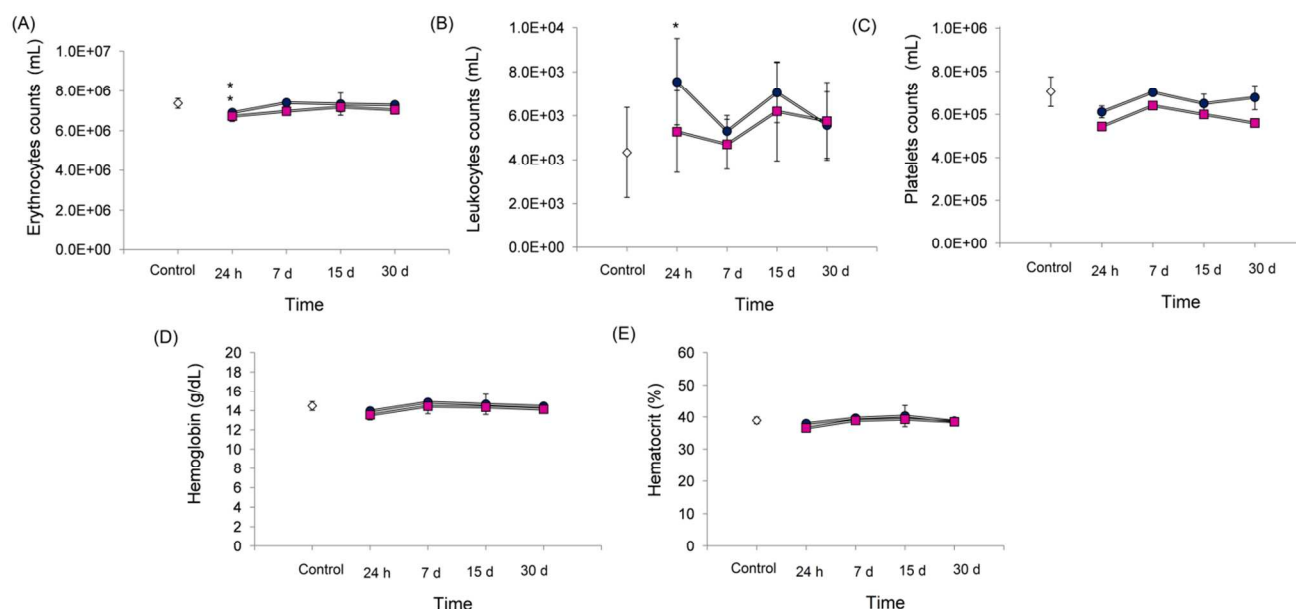


**Figure 6.** The effect of NP-DMSA and NP-PEG-(NH<sub>2</sub>)<sub>2</sub> on hematological parameters. (A) Erythrocytes, (B) Leukocytes, (C) Platelets, (D) Hemoglobin and (E) Hematocrit in Wistar rats after a single dose of 2.5 mg/kg. Values represent mean  $\pm$  SD (n=4). (\*) marks significant differences between bioferrofluids and control. Control animals were sacrificed progressively during the study and the values were averaged and represented with their standard deviation. Control [□], NP-DMSA [■], NP-PEG-(NH<sub>2</sub>)<sub>2</sub> [■].

### Citotoxicity test

Bone marrow has been used for evaluation of micronucleus frequencies *in vivo* in rodents in genotoxic risk characterization but also as a citotoxicity test<sup>32, 34, 35</sup>. This tissue has the most active cell division, therefore mutagenic or toxic effects of drugs or other chemicals can cause diseases like aplastic anemia, which manifests as the cessation of normal blood cell production; or leukemias, that produce excessive hematologic cancer cells<sup>36</sup>.

In this study the ratio of polychromatic to normochromatic erythrocytes (PCE, NCE) was scored and the %PCE was determined according to the formula described in the Methods section. Thus, no significant differences were observed between the animals treated

and the corresponding control groups (Figure 7B), indicating that these bioferrofluids do not affect erythropoiesis or cell proliferation of polychromatic erythrocytes in the bone marrow at the analyzed dose.

### Conclusions

Uniform magnetite nanoparticles coated with dimercaptosuccinic acid (DMSA) and polyethylene glycol (PEG) have been used in this work to assess their hematotoxicity, evaluating the blood toxicity *in vitro* and *in vivo* in a rat model.

## ARTICLE

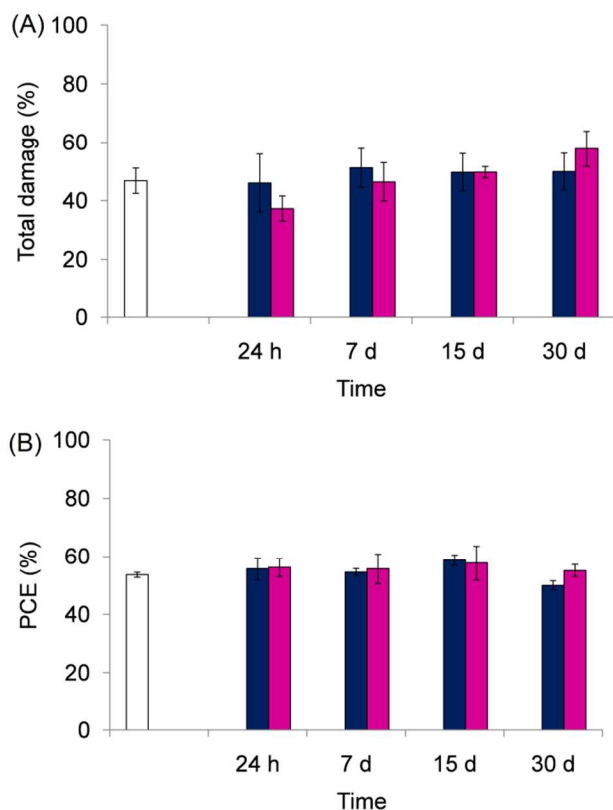


**Figure 7.** Comet assay of blood samples and Micronucleus test of bone marrow samples. (A) Total damage observed after nanoparticles administration. (B) Ratio of immature to mature erythrocytes observed after nanoparticles administration at a dose of 2.5 mg/kg B.W. Values represent mean  $\pm$  SD (n=4). Dunnett's test; significant differences with  $p < 0.05$ . Control [□], NP-DMSA [■], NP-PEG-(NH<sub>2</sub>)<sub>2</sub> [■]

The *in vitro* analysis consists on global plasma coagulation tests (PT, aPTT, Fibrinogen) and platelet aggregation while the hematotoxicity studies *in vivo* include a complete blood count and the possible genotoxic effects analysis in the hematopoietic function of the bone marrow. *In vitro* analyses reveal prolonged aPTT values for NP-DMSA compared with PEG-coated nanoparticles, which indicate higher anticoagulant effect for the former, probably due to a higher surface charge and the formation of a protein corona. No significant

changes were observed in the cell count, nor hemolysis for both bioferrofluids.

The *in vivo* tests showed that these bioferrofluids do not cause genotoxic effects and do not affect erythropoiesis or increase the number of immature erythrocytes in the bone marrow at the analyzed dose. However, nanoparticles administration showed a significant effect on the leukocytes counts in animals treated with DMSA coated nanoparticles 24 h after injection. This response is not observed in animals treated with PEG modified nanoparticles which justifies the use of this polymer in biomasking strategies.

### Acknowledgements

L.M.A.A. acknowledges financial support from the Spanish Ministry of Science and Innovation FPI research grants. Technical support from the University Hospital Lozano Blesa, Zaragoza, Spain and from María Angeles Gracia, Ana Isabel Martínez de Ternero, Maria Rosa Borrell Sanz. AR holds a predoctoral fellowship from a CSIC-CITMA collaborative project (B01CU2009; ICM, 2011-2014) and a short-term fellowship from CNPq (DTI-2; 383934/2013-3). This work was partially supported by grants from the Spanish Ministry of Economy and Competitiveness (MAT2011-23641 and MAT2011-25991).

### Notes and references

<sup>a</sup>Instituto de Ciencia de Materiales de Madrid, Departamento de Biomateriales y Materiales Bioinspirados, CSIC, Sor Juana Inés de la Cruz 3, Cantoblanco, 28049, Madrid, Spain. Tel: +34 91 334 9000.

<sup>b</sup>Centro de Estudios Avanzados de Cuba, San Antonio de Los Baños km 3½, La Habana, Cuba.

## ARTICLE

<sup>c</sup>Instituto de Ciencia de Materiales de Aragón. CSIC-Universidad de Zaragoza, and Departamento de Física de la Materia Condensada. Facultad de Ciencias, 50009 Zaragoza, Spain. Tel: +34 976 76 24 61

<sup>d</sup>Universidade de Brasília, Departamento de Genética y Morfología, Campus Universitario Darcy Ribeiro, CEP 70910-900, Brasília DF, Brazil.

<sup>e</sup>Departamento de Medicina, Facultad de Medicina, Universidad de Zaragoza, 50009 Zaragoza. Spain.

Email: [puerto@icmm.csic.es](mailto:puerto@icmm.csic.es), [amillan@unizar.es](mailto:amillan@unizar.es)

<sup>§</sup> A. Ruiz and L.M.A. Ali y have contributed equality to this work.

- M. Colombo, S. Carregal-Romero, M. F. Casula, L. Gutierrez, M. P. Morales, I. B. Bohm, J. T. Heverhagen, D. Prospero and W. J. Parak, *Chemical Society reviews*, 2012, **41**, 4306-4334.
- W. H. Suh, K. S. Suslick, G. D. Stucky and Y. H. Suh, *Progress in neurobiology*, 2009, **87**, 133-170.
- V. Hirsch, C. Kinnear, M. Moniatte, B. Rothen-Rutishauser, M. J. D. Clift and A. Fink, *Nanoscale*, 2013, **5**, 3723-3732.
- S. I. Palma, M. Marciello, A. Carvalho, S. Veintemillas-Verdaguer, M. P. Morales and A. C. Roque, *Journal of Colloid Interface Science*, 2015, **437C**, 147-155.
- U. Wattendorf and H. P. Merkle, *Journal of pharmaceutical sciences*, 2008, **97**, 4655-4669.
- M. Lundqvist, J. Stigler, T. Cedervall, T. Bergga, M. B. Flanagan, I. Lynch, G. Elia and K. Dawson, *acs.nano*, 2011, **5**, 7503-7509.
- C. Chouly, L. Bordenave, R. Bareille, V. Guerin, A. Baguey, D. Poulighen, C. Baguey and P. Jallet, *Clinical Materials*, 1994, **15**, 293-301.
- M. A. Dobrovolskaia, J. D. Clogston, B. W. Neun, J. B. Hall, A. K. Patri and S. E. McNeil, *Nano Letters*, 2008, **8**, 2180-2187.
- A. Ruiz, Y. Hernández, C. Cabal, E. González, S. Veintemillas-Verdaguer, E. Martínez and M. P. Morales, *Nanoscale*, 2013, **5**, 11400-11408.
- L. M. A. Ali, M. Gutiérrez, R. Cornudella, J. A. Moreno, R. Piñol, L. Gabilondo, A. Millán and F. Palacio, *Journal of Biomedical Nanotechnology*, 2013, **9**, 1272-1285.
- A. Mayer, M. Vadon, B. Rinner, A. Novak, R. Wintersteiger and E. Frohlich, *Toxicology*, 2009, **258**, 139-147.
- N. Gulati, R. Rastogi, A. K. Dinda, R. Saxena and V. Koul, *Colloids and Surfaces B: Biointerfaces*, 2010, **79**, 164-173.
- Z. Yang, W. Zhang, J. Zou and W. Shi, *Polymer*, 2007, **48**, 931-938.
- B. W. Neun and M. A. Dobrovolskaia, in *Method for in vitro analysis of nanoparticle thrombogenic properties*, ed. S. E. McNeil, Springer Science+Business Media, 2011, pp. 225-235.
- Y. X. Wang, *Quantitative imaging in medicine and surgery*, 2011, **1**, 35-40.
- A. Ruiz, G. Salas, M. Calero, Y. Hernández, A. Villanueva, F. Herranz, S. Veintemillas-Verdaguer, E. Martínez, D. F. Barber and M. P. Morales, *Acta biomaterialia*, 2013, **9**, 6421-6430.
- A. Ruiz, P. C. Morais, R. B. Azevedo, Z. G. M. Lacava, A. Villanueva and M. P. Morales, *Journal of Nanoparticle Research*, 2014, **16**.
- M. T. Zhu, W. Y. Feng, B. Wang, T. C. Wang, Y. Q. Gu, M. Wang, Y. Wang, H. Ouyang, Y. L. Zhao and Z. F. Chai, *Toxicology*, 2008, **247**, 102-111.
- R. Fernández-Pacheco, C. Marquina, J. G. Valdivia, M. Gutiérrez, M. S. Romero, R. Cornudella, A. Laborda, A. Vilorio, T. Higuera, A. García, J. A. G. d. Jalón and M. R. Ibarra, *Journal of Magnetism and Magnetic Materials*, 2007, **311**, 318-322.
- D. Simberg, W. M. Zhang, S. Merkulov, K. McCrae, J. H. Park, M. J. Sailor and E. Ruoslahti, *Journal of Control Release*, 2009, **140**, 301-305.
- S. Sun and H. Zeng, *Journal of the American Chemical Society*, 2002, **124**, 8204-8205.
- S. Sun, H. Zeng, D. B. Robinson, S. Raoux, P. M. Rice, S. X. Wang and G. Li, *Journal of American Chemical Society*, 2004, **126**, 273-279.
- R. Mejías, L. Gutiérrez, G. Salas, S. Pérez-Yagüe, T. M. Zotes, F. J. Lázaro, M. P. Morales and D. F. Barber, *Journal of Controlled Release*, 2013, **171**, 225-233.
- N. P. Singh, M. T. McCoy, R. R. Tice and E. L. Schneider, *Experimental Cell Research*, 1988, **175**, 184-191.
- M. C. Gontijo, Á. Marques and R. Tice, in *Teste do cometa para a detecção de dano no DNA e reparo em células individualizadas*, eds. L. Ribeiro, D. Salvadori and E. Marques, Canoas: ULBRA, 2003, pp. 247-279.
- P. Jalszyński, M. Kujawski, M. Czub-Świerczek, J. Markowska and K. Szyfter, *Mutation Research/DNA Repair*, 1997, **385**, 223-233.
- M. Mahmoudi, A. M. Abdelmonem, S. Behzadi, J. H. Clement, S. Dutz, M. R. Ejtehad, R. Hartmann, K. Kantner, U. Linne, P. Maffre, S. Metzler, M. K. Moghadam, C. Pfeiffer, M. Rezaei, P. Ruiz-Lozano, V. Serpooshan, M. A. Shokrgozar, G. U. Nienhaus and W. J. Parak, *ACS Nano*, 2013, **7**, 6555-6562.
- Z. Ademovic, B. Holst, R. A. Kahn, I. Jorring, T. Brevig, J. Wei, X. Hou, B. Winter-Jensen and P. Kingshott, *Journal of materials science. Materials in medicine*, 2006, **17**, 203-211.
- M. F. Song, Y. S. Li, H. Kasai and K. Kawai, *Journal of clinical biochemistry and nutrition*, 2012, **50**, 211-216.
- M. Boettcher, S. Grunda, S. Keiter, T. Kosmehl, G. Reifferscheid, N. Seitz, P. S. Rocha, H. Hollert and T. Braunbeck, *Mutation research*, 2010, **700**, 11-17.
- M. Z. Vasquez, *Mutagenesis*, 2010, **25**, 187-199.
- D. E. Bowen, J. H. Whitwell, L. Lillford, D. Henderson, D. Kidd, S. McGarry, G. Pearce, C. Beevers and D. J. Kirkland, *Mutation Research/ Genetic Toxicology and Environmental Mutagenesis*, 2011, **722**, 7-19.
- G. Krishna and M. Hayashi, *Mutation Research/Fundamental and Molecular Mechanism of Mutagenesis*, 2000, **455**, 155-166.
- A. T. Doherty, J. E. Hayes, J. Molloy, C. Wood and M. R. O'Donovan, *Toxicology Research*, 2013, **2**, 321.
- H. Holden, J. B. Majeska and D. Studwell, *Mutation Research/Genetic Toxicology and Environmental Mutagenesis*, 1997, **391**, 87-89.
- R. Snyder, *Annals of the New York Academy of Sciences*, 2014, **1310**, 1-6.